Contract No.:

This manuscript has been authored by Savannah River Nuclear Solutions (SRNS), LLC under Contract No. DE-AC09-08SR22470 with the U.S. Department of Energy (DOE) Office of Environmental Management (EM).

Disclaimer:

Pressurization Analysis for Heating of a Screw Top Utility Can Loaded with Plutonium Oxide Powder by a 1273 K Fire

James E. Laurinat[1]
Savannah River National Laboratory
Savannah River Site
Aiken, South Carolina 29808
james.laurinat@srnl.doe.gov
Matthew R. Kesterson
Savannah River National Laboratory
Savannah River Site
Aiken, South Carolina 29808
matthew.kesterson@srnl.doe.gov
Steve J. Hensel
Savannah River Nuclear Solutions LLC
Savannah River Site
Aiken, South Carolina 29808
steve.hensel@srnl.doe.gov
ASME Fellow

ABSTRACT

The documented safety analysis for the Savannah River National Laboratory (SRNL) evaluates the consequences of a postulated 1273 K fire in a glovebox. The radiological dose consequences for a pressurized release of plutonium oxide powder during such a fire depend on the maximum pressure that is attained inside the oxide storage containers. The oxide storage configuration selected for analysis is can/bag/can, comprised of oxide powder inside an 8.38×10^{-6} m^3 stainless steel B vial inside 0.006 kg of polyethylene bagging inside a one-quart screw top utility can of the type commonly used to package solvents or rubber cements.

To enable evaluation of the dose consequences, temperature and pressure transients have been calculated for exposure of a typical set of storage containers to the fire. The pressurization analysis credits venting to and from the B vial but does not credit venting or leakage from the can. Due to the low rate of venting from the B vial into the can gas space, the can pressure is nearly independent of the B vial pressure.

Calculated maximum pressures are compared to the utility can burst pressure. In lieu of a structural analysis of the utility cans, burst pressures and leakage rates were measured using compressed nitrogen gas. The measured gauge burst pressure was 2.50×10^5 +/- 0.43×10^5 Pa. The measured burst pressures are lower than the calculated maximum pressure due to fire exposure, indicating that the utility cans could burst during exposure to a 1273 K fire.

[1] Corresponding author

.

INTRODUCTION

The Savannah River National Laboratory (SRNL) safety basis utilizes a graded approach to evaluate the radiological dose consequences of a pressurized release of plutonium dioxide powder during a postulated fire in a glovebox. The consequences depend on the maximum venting pressure and the amount of powder that is released. To provide input for the dose consequence evaluation, pressure transients and venting rates are analyzed for the exposure of a screw top utility can containing a standard cylindrical oxide storage vial called a B vial to a 1000 °C (1273 K) fire. During the fire the vial pressurizes due to heating and evaporation of moisture adsorbed onto the oxide powder that it contains. Venting occurs through a threaded connection between the vial cap and body. The threaded connection sometimes is sealed by an O-ring, which would fail during the early stages of the fire. If the O-ring is absent, the top surface of the threaded portion of the body abuts against the cap. The rate of venting in this case is limited by the clearance between the cap and body surfaces. Venting from the can occurs through the screw top threads and, at higher pressures, along the can seams. The rate of venting from the can is measured rather than calculated from dimensional analysis.

Heat transfer during the fire exposure is modeled using COMSOL Multiphysics®, a finite element code. It is assumed that the rate of heat transfer is determined by the rate of thermal radiation and natural and forced convection to the screw top utility can surfaces. Rates of heat transfer are computed for upright or recumbent cans and vials, either engulfed by the fire or exposed to the fire over half the vial circumference.

The pressurization analysis is performed separately in a Microsoft Excel® spreadsheet macro, using tabulated results from the heat transfer calculation. The pressurization analysis includes a correction to account for cooling of the oxide powder due to evaporation of the adsorbed moisture.

B VIAL AND SCREW TOP CAN DESCRIPTIONS

The B vial has a diameter of 1.0 in. (0.0254 m) and a total height of 1.687 in. (0.0428 m). The B vial capacity is 8.38×10^{-6} m^3. The B vial is constructed of 304L stainless steel. The B vial has a threaded cap. The threads are Unified Fine (UNF), 14 threads per in. (551 threads per m), with a nominal diameter of 0.875 in. (0.0222 m) along the threads. The threads are sealed with a nitrile rubber O-ring that spans the gap between the cap and body. The O-ring is a Parker size 2-116-70, with an inner diameter of 0.737 in. (0.0187 m), a thickness of 0.103 in. (0.00262 m), and a Shore hardness rating of 70.

The screw top can is a 401 x 406 (4 1/16 in. (0.1032 m) diameter by 4 3/8 in. (0.1111 m) high) screw neck type can manufactured by Consolidated Can of Paramount, California. The capacity of an empty screw top can is 8.49×10^{-4} m^3. The can has dry, no solder seams at the top and bottom and along one circumferential side. Figure 1 shows a B vial, with the O-ring in place, and the screw top can.

For the fire exposure analysis, it is assumed that the can contains one B vial and 0.006 kg of polyethylene bagging. The B vial is assumed to contain 0.005 kg of PuO_2, with adsorbed moisture totaling 5% of the oxide weight. During the fire exposure, it is assumed that the polyethylene bagging forms a melt pool at the bottom of the can. To avoid the complications of moving boundaries inside the can, the analysis assumes that the melt pool geometry exists at the start of the fire.

® COMSOL Multiphysics is a registered trademark of COMSOL AB.

® Microsoft Excel is a registered trademark of Microsoft Corporation of Redmond, Washington.

HEAT TRANSFER ANALYSIS

The temperature transients for the screw top can, the B vial, and their contents are calculated using Version 4.3 of COMSOL Multiphysics®. The finite element model assumes that the can is heated by a 1000 °C (1273 K) fire on its circumference. An accurate geometric model of the vial consisting of the 304L stainless steel body, the nitrile rubber O-ring, and the plutonium oxide powder contents was constructed. Also included in the model is an air gap above the oxide layer.

The finite element simulation models heat conduction within the stainless steel body, the oxide, and the O-ring, and between their surfaces. The model accounts for heat transfer across the air gaps inside the can and the vial by conduction and thermal radiation. Heat transfer from the fire to the can is modeled by including thermal radiation and forced convection. The emissivity for the stainless steel surfaces is set conservatively at 0.9, which is a value typical for soot-covered surfaces. [1] The O-ring emissivity is set at 0.94. [2] The heat transfer coefficient for the outside surfaces is evaluated using the Polhausen correlation for flow past a surface with a leading edge. [3] The thermal radiation boundary condition is applied to all surfaces of the recumbent can and to all surfaces except the bottom surface of the upright can, which is assumed to be insulated. The convective heat transfer model is applied only to the circumferential surfaces of both the upright and recumbent cans. The characteristic length for the heat transfer correlation is the height of the upright can and the diameter of the recumbent can. Exposure of one side of the can to the fire is modeled by assuming that heat transfer over half of the circumference is to air at the initial ambient temperature. The top of the upright can and the end surfaces of the recumbent can are assumed to be exposed to the fire, both for cases where the fire engulfs the entire can surface and where only one side of the can is exposed to the fire.

The thermal conductivity of the plutonium oxide powder is calculated using a Los Alamos National Laboratory (LANL) model that accounts for both conduction within and between the powder particles and thermal radiation between particles. [4,5] The properties of other materials are obtained primarily from tabulations of either default data built into COMSOL Multiphysics® or data from external sources. The density and heat capacity of the nitrile rubber O-ring are specified as 1000 kg/m^3 and 250 J/kg/K, and the O-ring thermal conductivity is set at 0.24 W/m/K. The plutonium oxide density is specified as 1800 kg/m^3, based on typical measured bulk densities for PuO_2 powders.

The total effective heat capacity for the oxide is computed as the sum of the intrinsic plutonium oxide powder heat capacity and an equivalent heat capacity for evaporation of adsorbed moisture:

$$c_{p,PuO_2,tot} = c_{p,PuO_2} + c_{p,PuO_2,ev} \tag{1}$$

A correlation for the intrinsic specific heat of plutonium dioxide was developed as part of an Oak Ridge National Laboratory (ORNL) study of mixed oxide fuel properties. [6] The equivalent heat capacity that corresponds to the latent heat required to evaporate adsorbed moisture up to its vapor pressure is given by

$$c_{p,PuO_2,ev} = \frac{\lambda_{H_2O}}{n_{H_2O}}\left(\frac{f_{H_2O}}{1-f_{H_2O}}\right)\frac{dn_{H_2O,ev}}{dT} \tag{2}$$

The following empirical expression is used to correlate the latent heat of water as a function of temperature at the moderate pressures present in the vial [7]

$$\lambda_{H_2O} = 1000\left(3335 - 2.91T\right) \tag{3}$$

The number of moles of water evaporated from the oxide powder is given by

$$n_{H_2O,ev} = \frac{min\left(P_{v,H_2O}, P_{max,H_2O}\right)V}{R_g T} \tag{4}$$

For $P_{v,H_2O} < P_{max,H_2O}$,

$$c_{p,PuO_2,ev} = \frac{\lambda_{H_2O} V}{n_{H_2O} R_g}\left(\frac{f_{H_2O}}{1-f_{H_2O}}\right)\frac{d}{dT}\left(\frac{P_{v,H_2O}}{T}\right) \tag{5}$$

and, for $P_{v,H_2O} \geq P_{max,H_2O}$,

$$c_{p,PuO_2,ev} = 0 \tag{6}$$

Venting reduces the rate of pressure increase in the B vial not only directly but also by evaporative cooling of the oxide. It is assumed that the amount of water vapor exiting the vent is accompanied by an equal molar amount of water vapor evaporating from the oxide surface. The amount of water vapor that exits the vent is related to the total vent flow rate by assuming that the gas inside the B vial is well-mixed, so that the noncondensable gas vent rate is equal to the total vent rate multiplied by the fraction of the gas space occupied by noncondensable gas; this gives a vent factor that is an exponential function of the volume of gas that has been vented. In addition, the effective oxide heat capacity is increased by the latent heat associated with the increase in the vapor pressure in excess of the pressure increase due to gaseous thermal expansion. The rate of temperature increase for the oxide, on which the rate of evaporation is based, is reduced by the product of the latent heat of vaporization and the sum of the venting rate for the vapor and rate of pressurization of the B vial gas space due to heating, divided by the product of the oxide mass and the effective heat capacity of the oxide, according to the following expression:

$$\left(\frac{dT}{dt}\right)_{ox,adj} = \frac{\left(\frac{dT}{dt}\right)_{ox} - \frac{\rho_{H_2O,v} kQ \lambda_{H_2O}\left(1-exp\left(-V_{vent}\right)\right)}{m_{PuO_2} c_{p,PuO_2}}}{1+\frac{\rho_{H_2O,v} V_{g,1} \lambda_{H_2O}}{m_{PuO_2} c_{p,PuO_2,adj}}\left(\frac{1}{P_{v,H_2O,ox,adj}}\left(\frac{dP_{v,H_2O}}{dT}\right)_{ox,adj} - \frac{1}{T_{ox,adj}}\right)} \tag{7}$$

PRESSURIZATION ANALYSIS

Pressurization due to Thermal Expansion and Evaporation in the B Vial

The total pressure change inside the B vial during the fire transient is calculated by summing the contributions from volumetric expansion and evaporation of adsorbed moisture and subtracting the contribution from venting. Heating of noncondensable gas and moisture evaporation combine to give the total increase in the pressure.

$$P_t = P_e + P_{H_2O} \tag{8}$$

The increase in pressure due to heating, P_e, is calculated from the ideal gas law. It is assumed that the gas space inside the vial remains saturated with water vapor at all times, including at the start of the fire transient, until all adsorbed moisture evaporates. Therefore, the increase in the vapor pressure during the fire transient is given by

$$P_{H_2O} = min\left(P_{v,H_2O} - P_{v,H_2O,0}, P_{max,H_2O}\right) \tag{9}$$

The maximum vapor pressure for evaporation of all water adsorbed on the plutonium dioxide is calculated using the ideal gas law. The water vapor pressure is given by an Antoine equation. [8]

Pressurization due to Expansion and Plastic Pyrolysis in the Can

As in the B vial, the rate of pressurization due to gas expansion in the can is based on the ideal gas law. The rate of pressurization due to plastic pyrolysis is computed using the rate of gas generation determined in the heat transfer analysis.

The dominant species of gas generated by the pyrolysis of the polyethylene bagging material is ethylene (C_2H_4), which is the monomeric unit of polyethylene. The heat of reaction for polyethylene is obtained by subtracting the heat of formation of polyethylene from the heat of formation of ethylene. The heats of formation for polyethylene and ethylene are -5.636×10^4 and 5.247×10^4 J/mol C_2H_4, respectively. [9] The polyethylene is not completely pyrolyzed; to account for incomplete pyrolysis, only half of the heat of formation for polyethylene is included in the calculation of the heat of pyrolysis. Therefore, the calculated heat of pyrolysis is 8.065×10^4 J/mol C_2H_4.

Although ethylene is the dominant gas species generated by polyethylene pyrolysis, the estimation of the number of moles of gas per gram of polyethylene also accounts for the presence of higher molecular weight pyrolysis products. The volumetric gas flow rate is calculated by dividing the rate of mass loss by pyrolysis by the average molecular weight of the pyrolysis products. The average molecular weight is correlated as a function of temperature using fluidized bed pyrolysis data over the temperature range from 773 K (500 °C) to 973 K (700 °C). [10] The fluidized bed residence time of approximately 15 s approximately matches the rate of pyrolysis calculated for exposure of the screw top can to the fire, so the distribution of product gases for the data should be representative of the distribution for the fire exposure. The average molecular weight of the pyrolysis gas is correlated with temperature by

$$y_M = exp\left(0.4892 - 10.502\left(\frac{T_{sg}}{1000}\right) + 13.512\left(\frac{T_{sg}}{1000}\right)^2 \right) \quad (10)$$

The intrinsic reaction rate for the pyrolysis of polyethylene was determined by isothermal and standard thermogravimetric pyrolysis measurements, respectively. [11] The reaction rate is expressed as an Arrhenius function of temperature. Because the pyrolysis reaction is endothermic, the rate of reaction is limited by the rate of heat transfer to the plastic surface. The limiting heat transfer rate is modeled as the sum of the maximum rates of thermal radiation and gaseous convection heat transfer to the plastic surface and conductive heat transfer from the screw top can container walls. The heat transfer area is approximated by assuming that the polyethylene bag melts and collects at the bottom of the screw top can. To bound rate of heat transfer by convection, the screw top can gas thermal conductivity is set at 150 W/m/K once pyrolysis starts. Computationally, pyrolysis is phased in between 617.5 K and 642.5 K (344 °C and 369 °C).

Initial Pressurization due to Radiolytic Hydrogen Generation

If the B vial is sealed with an O-ring, it is assumed that the B vial might pressurize due to radiolytic hydrogen generation. Accordingly, an additional set of calculations with an initial positive gauge pressure is included to account for this possibility. Hydrogen backpressure measurements performed by Duffey and Livingston [12] indicate that, for a limited amount of

moisture adsorbed onto weapons grade plutonium oxide, the maximum gauge pressure due to hydrogen generation is about 5.65 x 10^5 Pa. This maximum pressure is in approximate agreement with the DOE 3013 Standard, [13] which states that the primary source of pressurization is radiolytic hydrogen and that the hydrogen gauge pressure is less than 100 psig (6.89 x 10^5 Pa). The screw top can is not sealed and therefore will not pressurize due to generation of radiolytic hydrogen.

Effect of Venting on Pressure

The adjusted pressure increase due to venting is computed by applying implicit time differencing. The implicit differencing equation takes the form

$$P_{t,adj,j+1} = \left(\frac{P_{t,adj,j} + P_a + P_{t,j+1} - P_{t,j}}{1 + \left(t_{j+1} - t_j\right) \frac{kA_x M_0 c}{V}} \right) - P_a \tag{11}$$

The second term in the denominator of Equation 11 accounts for the effect of the vent flow. The flow term is multiplied by the heat capacity ratio to account for the pressure-volume work performed by the venting gases. The heat capacity ratio is estimated under the assumption that, because the principal component of the gas mixture in the vial at pressures significantly above atmospheric is water vapor, the venting is equivalent to adiabatic expansion of slightly superheated steam. The heat capacity ratio is assigned a value of 1.2, which is between the value of 1.135 for polytropic expansion of saturated (wet steam) and 1.3 for adiabatic expansion of superheated (dry) steam. [14]

The vent flow rate is evaluated using the isothermal compressible flow equation, with a heat capacity ratio of 1.2. The friction factor for the compressible flow equation is computed as the sum of the laminar friction factor based on the vent channel length and hydraulic diameter and the Von Karman correlation for turbulent flow, with the roughness factor arbitrarily set at 0.001. [15] The entrance loss is modeled using a factor recommended by Zuk et al. [16] The compressible flow equation is solved iteratively, using Newton's method with a damping factor of 0.5.

The adjustment of the screw top can pressure for venting is computed by a second implicit finite difference equation that account for venting out of the can. This equation, which is applied successively, takes the form

$$P_{t,adj,2a,j+1} = \frac{P_{t,adj,2,j+1}}{1 + \left(t_{j+1} - t_j\right) \left(\frac{\beta_{test} V_{g,2.test} f_p \mu_{N_2,test}}{V_{g,2} \mu_{C_2H_4}} \right)} \tag{12}$$

Venting from the screw top can is modeled using a time constant because the pressure decreased exponentially with time during the can venting tests.

The term f_p conservatively accounts for choked flow during the can venting tests by setting the maximum, or initial pressure, for the venting tests equal to the minimum pressure for choked flow at the vent. With this assumption,

$$f_p = \left(\frac{P_{t,2,adj,j+1} + P_a}{P_{i,test}} \right)^2 \frac{P_{i,test} - P_a}{P_{t,2,adj,j+1}} \tag{13}$$

MODELING OF VENT PATHS

Venting through the B Vial O-rings

For venting of B vials with O-rings, the limiting vent path is assumed to follow the root of the threads between the body and cap of the vial. The threads are Unified Fine (UNF), 14 threads per in. (551 threads per m), with a nominal diameter of 0.875 in. (0.0222 m) along the threads. Standard thread design calls for rounded clearances between the troughs and the peaks of each thread. At the clearances, the peaks are truncated to flat surfaces, equal to 0.125 times the thread pitch at the outer thread peak and 0.250 times the thread pitch at the inner thread peak. The troughs are rounded to provide a clearance opposite the truncated peaks. It is assumed that the rounded clearances take the shape of a circular chord section that spans a 120-degree arc. The analysis credits only the flow through the larger inner thread clearance, which has a hydraulic diameter of 1.68×10^{-4} m.

The analysis for venting through the gap at the thread tip accounts for possible partial pluggage of the flow path by oxide powder particles. It is envisioned that fine particle entrainment could reduce the cross-sectional area of the vent channel to a proportion equal to the void fraction of the bulk powder. The cross-sectional area for partially plugged flow is obtained by multiplying the cross-sectional area by the void fraction in the bulk oxide powder. The bounding value for the hydraulic diameter for flow in the vent channel is obtained by multiplying the hydraulic diameter for the open channel by the square root of the void fraction. The void fraction is set equal to 0.75, based on a comparison of the pycnometric density, 11460 kg/m^3, and the maximum bulk density of 1800 kg/m^3, with some allowance for intraparticle voids.

The O-ring release pressure is calculated from a force balance that accounts for elastic and frictional contact resistances. The O-ring would leak if the pressure in the B vial overcomes the O-ring's contact resistance and stretches it so that it is displaced from the gap between the cap and the body. The release pressure is given by

$$\Delta P_{rel} = \frac{\pi w_{oring} E(H)}{4 r_{oring}} \left(\frac{d_{vial} - 2 r_{oring}}{2 r_{oring}} \right) + f_s \Delta P_{leak} \tag{14}$$

The first term in this expression is the pressure required to stretch the O-ring, evaluated from a hoop stress analysis. It is assumed that the amount of stretch varies linearly with the differential pressure, with a constant of proportionality equal to Young's modulus. The Young's modulus is evaluated as a function of the O-ring hardness, by inverting the error function expression [17]

$$H = 100\, erf\left(0.0003186\, E(H)^{0.5}\right) \tag{15}$$

The nominal Shore hardness for the B vial O-ring is 70, with an approximate upper bound of 77 that accounts for stiffening of the O-ring rubber with increasing temperature. [18] To bound the leak pressure, the hardness is set at 77 up to the point where the nitrile rubber in the O-ring begins to soften. The reduction in the hardness at higher temperatures is estimated based on the hardness versus temperature variation for fluorosilicone rubber.

The second term in Equation 14 is the pressure needed to overcome static friction. The static friction is calculated as a function of the leak pressure using an empirical fit to measured static friction coefficients for plastic/metal surfaces. [19] The empirical fit is expressed as an error function to give an asymptotic approach to a maximum value of one at high leak pressures. Using an error function, the following expression is obtained:

$$f_s = erf\left(2.315\left(\frac{14.696}{\Delta P_{leak}}\right)\right) \quad (16)$$

The leak pressure and the static coefficient of friction are evaluated using a measured compression ratio. The compression ratio was determined by measuring the distance that the cap could be turned from first contact where the O-ring exactly fit the gap between the cap and body to hand tight. This distance was 5/32 in. (0.00397 m) measured along the perimeter of the cap. This turning distance translates to a compression ratio of 0.0345, given the cap diameter of 1.0 in. (0.0254 m) and the thread pitch of 14/in (551/m). For this compression ratio, the leak pressure at ambient temperature is calculated to be 6.29 x 10^5 Pa (91.2 psi) and the friction coefficient is computed to be 0.423. The variation of release pressure with temperature is shown by Figure 2.

Venting through Gap between the B Vial Cap and Body

In the absence of an O-ring, the hydraulic diameter for contact between the vial body and cap is calculated for a representative diamond-shaped space between two saw tooth surfaces. The peak-to-trough distance for the diamond-shaped gap is assumed to be four times the average surface roughness, which is 63 μin (1.6 x 10^{-6} m). Particle entrainment is not considered for flow in the gap between the vial body and cap surfaces in the absence of an O-ring, due to the small gap size and the high degree of tortuosity of the vent path.

Venting from Screw Top Cans

The rate of pressure decrease due to venting from the screw top cans is calculated directly using the results of leak tests, so no analysis of the can vent gaps is needed. Results of the leak tests are presented in the following section.

SCREW TOP CAN LEAK AND BURST TESTS

R&D Technology/Packaging Technology and Pressurized Systems conducted leak and burst tests to determine the leak rate and the burst pressure for the screw top cans. Physical tests were conducted in lieu of computational structural analyses due to the lack of design specifications for the cans. Physical tests also were performed to obtain uncertainty bounds for the burst pressure and the leak rate.

Both the burst and the leak tests were performed by placing the test can in a Lexan box that is routinely used for low pressure tests. The tests used compressed nitrogen from a cylinder. The compressed gas tubing was connected to the can by drilling a hole in the bottom of the can and installing a tubing connector through that hole. The tubing was then connected using a ferrule seal. During the burst tests, the pressure was slowly increased until the cans burst. For the leak tests, the gauge pressure was increased to a nominal level of 18.0 psig (1.24 x 10^5 Pa). When this pressure was reached, flow to the can was cut off by turning a ball valve and the rate of pressure decrease was electronically recorded. A blank leak test was conducted in which the can was replaced by a ball valve, which was opened at the initial gauge set pressure of 1.24 x 10^5 Pa. The rate of pressure decrease for the blank test was measured to verify that the rate of pressure drop was controlled solely by the leak rate through the can lid connection.

To obtain valid data, it was necessary to slightly alter the test apparatus and procedure. It was determined that the cans could not be pressurized to the burst pressure due to excessive leakage through the screw lid threads, even with the addition of a gasket between the top of the can body and the underside of the lid. Therefore, for the burst tests, the lid was brazed onto the

can. In addition, both the burst and leak tests required replacement of the existing 1/8-in. (0.00318-m) OD high pressure tubing connecting the can and the pressure supply tube to the pressure transducer with ¼-in. (0.00635-m) OD, 0.035-in. (0.000889-m) wall tubing to eliminate pressure differences between the transducer and the can. With these changes, the tests were conducted successfully.

Three cans were tested during both the burst and leak tests. For each leak test, the lid was screwed onto the can while holding both the can body and the lid in standard bayonet-style glovebox gloves. The lid was screwed on as tight as possible without applying excessive force. Three leak test trials were conducted for each can, for a total of nine leak tests.

Leak Test Results

For the nine can leak tests that were run, a preliminary analysis showed that the differences in the average time constants for each can did not differ significantly. Consequently, all nine tests were analyzed as a single group. The Life Distribution tool within JMP® was utilized to determine the best fit probability distribution for the time constants. This tool applies the Akaike information criterion, corrected for small sample sizes (AICc). [20,21] By a statistically significant margin, the threshold, or three-parameter, Weibull function [22] gave the best fit. The threshold time constant for this distribution is 0.424 1/s. The time constant used in the venting analysis is the 95% lower likelihood bound to this time constant, which is 0.414 1/s. This lower bound and the maximum initial pressure for the tests are used to construct the asymptote shown in Figure 3.

Burst Test Results

Three successful bursts tests were conducted. In all these tests, the cans burst along the soldered seam that runs from the bottom to the top of the can body along the circumferential side, as shown by Figure 4. Bulging of the cans was visible starting about 10 psi (6.9×10^4 Pa) below the burst pressure, particularly on the can bottom and at the top of the lid.

Figure 5 plots the pressure transients for the burst tests. It may be noted that the pressure dropped very rapidly after Cans 3 and 4 burst, but much more slowly after Can 5 burst. This behavior is confirmed by the photos in Figure 4, which show that only a small gap developed at the solder joint for Can 5.

The gauge burst pressures, taken to be the maximum pressures shown in Figure 5, were 2.39×10^5, 2.64×10^5, and 2.48×10^5 Pa for Tests 3, 4, and 5, respectively. Based on these three tests, the average gauge burst pressure is 2.50 x E5 Pa, with a 90% confidence that the gauge burst pressure for any given can is between 2.07×10^5 and 2.93×10^5 Pa. The confidence interval is based on a Student's t statistic. These measured burst pressures bound the burst pressures during exposure to a fire, because the can strength degrades at elevated temperatures.

DISCUSSION OF RESULTS

Figure 6 illustrates the results of the heat transfer analyses for an upright screw top can after 20 s exposure to an engulfing 1000 °C (1273 K) fire. The temperature profile is taken prior to the peak pyrolysis rate. As this profile indicates, the oxide remains considerably cooler than the either the screw top can or the gas space inside the screw top can, due to its low thermal conductivity and high thermal mass. The polyethylene bagging material also remains relatively cool due to the endothermic nature of the pyrolysis reaction.

® JMP is a registered trademark of SAS Institute, Inc., of Cary, North Carolina.

Temperature and pressure transients for the same heat transfer case are plotted in Figures 7 and 8. A comparison of the temperature and pressure transients indicates the average plastic temperature plateaus between 400 °C (673 K) and 500 °C (773 K) at the same time that the screw top can pressure increases significantly. This signifies that the rate of pyrolysis is controlled by the rate of heat transfer to the plastic surface, so that the temperature remains relatively constant. It may be noted that after approximately 15 s the can and can gas temperatures drop, while the B vial temperatures rise sharply. These temperature changes result from the computationally stipulated increase in the can gas thermal conductivity to 150 W/m/K at the onset of the polyethylene pyrolysis. The model triggers the onset of pyrolysis over a 25-K plastic temperature interval centered at 630 K (357 °C).

The plotted pressure transients indicate that increases in the B vial pressure result from evaporation of adsorbed moisture, as the pressure rises occur concurrently with increases in the adjusted oxide temperature. Gas generation due to evaporation of adsorbed moisture inside the B vial has little if any effect on the screw top can pressure because of the relatively small volume of the B vial gas space compared to the screw top can gas space. Consequently, only a single screw top can pressure transient is plotted. The can pressure spikes at the same time as the plastic temperature plateaus due to pyrolysis. The model assumes that the can gauge pressure drops to zero once the maximum gauge burst pressure of 2.93×10^5 Pa is reached.

Table 1 lists the maximum calculated internal pressures for the B vial when the outer surface of the can is exposed to a 1000 °C (1273 K) fire. Maximum internal B vial gauge pressures range from 3.20×10^5 Pa, for a B vial without an O-ring inside an initially unpressurized upright can engulfed by fire, to 9.85×10^5 Pa, for a B vial with an O-ring and a partially blocked vent path inside an upright can fully engulfed by the fire when that B vial is initially pressurized to 82 psig (5.65×10^5 Pa). The screw top can is predicted to reach its maximum estimated gauge burst pressure of approximately 2.93×10^5 Pa ± the pressure change over one time step in all cases.

CONCLUSIONS

The maximum internal pressure for exposure of a screw top can containing 0.006 kg of polyethylene bagging and a B vial to a 1000 °C (1273 K) fire is equal to the measured can gauge burst pressure of 36.3 ± 6.3 psig (2.50×10^5 +/- 0.43×10^5 Pa). The primary source of pressurization is the generation of gases by pyrolysis of the polyethylene bagging inside the screw top can.

The maximum internal gauge pressure inside the B vial is calculated to be 9.85×10^5 Pa, for an upright can engulfed by flames, when the B vial is sealed by an O-ring and the O-ring vent path is partially blocked. This maximum pressure increase is significantly less than the increase in the gauge pressure previously calculated for exposure of a bare B vial to a 1000 °C (1273 K) fire, which was 215 psig (1.48×10^6 Pa), [4] so the consequences of the exposure of the screw top can to the fire are bounded by the consequences of the exposure of a B vial to the fire.

ACKNOWLEDGMENT

The assistance of G. L. Crow, D. J. Trapp, and E. P. Shine is greatly appreciated. G. L. Crow and D. J. Trapp conducted the screw top can burst and leak tests in the SRNL High Pressure Laboratory. E. P. Shine performed the statistical analysis of the vent test data.

FUNDING

Savannah River Nuclear Solutions, LLC (Contract No. DE-AC09-08SR22470; Funder ID: 10.13039/100008972) with the U.S. Department of Energy.

NOMENCLATURE

A,B,C	Antoine equation parameters
c	speed of sound for gas, m/s
c_{p,PuO_2}	specific heat for solid plutonium oxide, J/kg/K
$c_{p,PuO_2,adj}$	total effective specific heat for plutonium oxide powder at adjusted oxide temperature, J/kg/K
$c_{p,PuO_2,ev}$	contribution of moisture evaporation to the effective specific heat for plutonium oxide powder, J/kg/K
$c_{p,PuO_2,tot}$	total effective specific heat for plutonium oxide powder with adsorbed moisture, including evaporation effects, J/kg/K
d_{vial}	B vial outer diameter, m
$E(H)$	modulus of elasticity for the O-ring material, Pa
f_{H_2O}	mass fraction of the plutonium oxide that is adsorbed moisture
f_p	correction factor for choked flow venting at high pressures
f_s	coefficient of static friction for contact between rubber and steel
H	Shore hardness for nitrile rubber
k	gas heat capacity ratio
M_0	Mach number for gas flow reference to stagnation pressure
m_{H_2O}	mass of adsorbed water, kg
m_{PuO_2}	mass of plutonium oxide, kg
n_{H_2O}	number of moles of water adsorbed onto plutonium oxide
$n_{H_2O,ev}$	number of moles of water evaporated from plutonium oxide
P	pressure, Pa (psi)
$\left(\frac{dP}{dt}\right)_e$	rate of pressure increase due to volumetric expansion of gas inside the vial at the start of the fire, Pa/s (psi/s)
P_0	pressure inside the vial prior to the fire, Pa (psia), assumed to be ambient pressure
P_e	pressure inside the vial due to volumetric expansion, Pa (psia)
ΔP_{leak}	minimum differential pressure for leaking across the O-ring, Pa (psi)
P_{max,H_2O}	maximum water vapor pressure if all adsorbed water evaporates, Pa (psi)
ΔP_{rel}	differential pressure for release of the O-ring from its seat, Pa (psi)
P_{v,H_2O}	water vapor pressure, Pa (psia)
P_{H_2O}	pressure increase due to evaporation during the fire transient, Pa (psi)

P_t total increase in gauge pressure due to volumetric expansion and evaporation, Pa (psig)

$P_{t,adj,j}$ B vial gauge pressure at previous time step, adjusted for venting, Pa (psig)

$P_{t,adj,j+1}$ B vial gauge pressure at current time step, adjusted for venting, Pa (psig)

$P_{t,adj,2,j+1}$ screw top can gauge pressure at current time step, prior to adjustment for venting, Pa (psig)

$P_{t,adj,2a,j+1}$ screw top can gauge pressure at current time step, adjusted for venting, Pa (psig)

$P_{v,H_2O,0}$ saturation water vapor pressure at temperature prior to fire exposure, Pa (psi)

$P_{v,H_2O,ox,adj}$ water vapor pressure in the B vial at the adjusted oxide temperature, Pa (psi)

$\left(\frac{dP_{v,H_2O}}{dT}\right)_{ox,adj}$ rate of change of water vapor pressure in the B vial at the adjusted oxide temperature, Pa/K (psi/K)

Q volumetric vent flow rate, m^3/s

R_g ideal gas law constant, $m^3Pa(\ psia)/mol/K$

r_{oring} radius of the B vial O-ring groove, m

T temperature, K

$T_{ox,adj}$ oxide temperature, adjusted for cooling by evaporation, K

T_r reference temperature, 273.15 K

T_{sg} pyrolysis gas temperature, K (°C)

$\left(\frac{dT}{dt}\right)_{ox,adj}$ rate of temperature increase for oxide, adjusted for additional evaporation due to venting, K/s

$\left(\frac{dT}{dt}\right)_{ox}$ rate of temperature increase for oxide, from heat transfer analysis, K/s

t duration of exposure to fumes from the fire, s

V interior gas space in the B vial or can, m^3

$V_{g,1}$ gas space volume inside the screw top can during the fire, m^3

$V_{g,2,test}$ volume of gas space inside the screw top can and associated tubing during the venting tests, m^3

V_{vent} number of volumes of gas that have vented from the B vial

w_{oring} width of the O-ring prior to compression at ambient temperature, m

y_M ratio of pyrolysis gas molecular weight to ethylene molecular weight (0.028 kg/mol)

λ_{H_2O} heat of vaporization for water, J/kg

$\rho_{H_2O,v}$ water vapor density kg/m^3

ρ_{max,H_2O} water vapor density from evaporation if all adsorbed moisture evaporates, kg/m^3

$\mu_{C_2H_4}$ viscosity of ethylene gas at the vent, kg/m/s

$\mu_{N_2,test}$ viscosity of nitrogen for the venting test, kg/m/s

REFERENCES

[1] DOE-HDBK-3010-94, 1994, "DOE Handbook: Airborne Release Fractions/Rates and Respirable Fractions for Nonreactor Nuclear Facilities."

[1] U.S. Department of Energy, 1994, "DOE Handbook: Airborne Release Fractions/Rates and Respirable Fractions for Nonreactor Nuclear Facilities," U.S. Department of Energy, Washington, DC, Standard No. DOE-HDBK-3010-94.

[2] Giants, T. W., 2001, "Viton® GLT O-ring Resilience Study," The Aerospace Corporation Report No. TR-2001(1413)-4, U. S. Air Force Space and Missile Systems Center Report No. SMC-TR-02-25.

[3] Byrd, R. B., Stewart, W. E., and Lightfoot, E. N., 1960, Transport Phenomena, John Wiley & Sons, Inc., New York, p. 410.

[4] Laurinat, J. E., Kesterson, M. R., and Hensel, S. J., 2015, "Analysis of Pressurization of Plutonium Oxide Storage Vials during a Postulated Fire," Proceedings of the ASME 2015 Pressure Vessels & Piping Division Conference, Boston, Massachusetts, Paper PVP2015-45239.

[5] Bielenberg, P. A., Prenger, F. C., Veirs, D. K., and Jones, G. F., 2006, "Effects of Pressure on Thermal Transport in Plutonium Oxide Powder," Int. J. Heat Mass Tran., 49, 3229-3239.

[6] Carbajo, J. J., Yoder, G. L., Popov ,S. G., and Ivanov, V. K., 2001, "A Review of the Thermophysical Properties of MOX and UO_2 Fuels," J. Nucl. Mater., 299, 181-198.

[7] Smith, A. W., 1907, "Heat of Evaporation of Water," Phys. Rev. (Series I), 25, 145-170.

[8] Dortmund Data Bank Software and Separation Technology GmbH, 2020, "Saturated Vapor Pressure Calculations by Antoine Equation," Dortmund Data Bank Software and Separation Technology GmbH, Oldenburg, Germany, accessed Nov. 25, 2020. http://ddbonline.ddbst.com/AntoineCalculation/AntoineCalculationCGLexe?component=water.

[9] Splitstone, P. L., and Johnson, W. H., 1974, "The Enthalpies of Combustion and Formation of Linear Polyethylene," J. Res. NBS A Phys. Ch., 78A(5), 611-616.

[10] Williams, P. T., and Williams, E. A., 1999, "Fluidised Bed Pyrolysis of Low Density Polyethylene To Produce Petrochemical Feedstock," J. Anal. Appl. Pyrol., 51, 107-126.

[11] Ceamanos, J., Mastral, J. F., Millera, A., and Aldea, M. E., 2002, "Kinetics of Pyrolysis of High Density Polyethylene. Comparison of Isothermal and Dynamic Experiments," J. Anal. Appl. Pyrol., 65, 93-110.

[12] Duffey, J. M., and Livingston, R. M., 2002, "Gas Generation Testing of Plutonium Dioxide," Fifth Topical Meeting on Spent Nuclear Fuel and Fissile Materials Management, Charleston, South Carolina, September 17-20, 2002, WSRC-MS-2002-00705.

[13] U.S. Department of Energy, 2012, "Stabilization, Packaging, and Storage of Plutonium-Bearing Materials," U.S. Department of Energy, Washington, DC, Standard No. DOE-STD-3013-2012, 2012.

[14] Gebhardt, G. F., 1917, Steam Power Plant Engineering, John Wiley & Sons, Inc., New York, p. 970.

[15] Green, D. W., 1984, Perry's Chemical Engineers' Handbook, 6th ed., 1984, McGraw-Hill, New York, p 5-24.

[16] Zuk, J., Ludwig, L. P., and Johnson, R. L., 1972, "Quasi-One-Dimensional Compressible Flow across Face Seals and Narrow Slots," NASA Technical Note TN D-6668, Lewis Research Center, Cleveland, Ohio.
[17] British Standards Institute, 1957, "Methods of Testing Vulcanized Rubber," 1957, British Standards, London, UK, Standard No. 903, Part A7.
[18] Parker Hannifan Corporation O-Ring Division, 2018, "Parker O-Ring Handbook", Parker Hannifan Corporation, Lexington, KY, Document No. ORD 5700.
[19] Deladi, E. L., 2006, "Static Friction in Rubber-Metal Contacts with Application to Rubber Pad Forming Processes," Ph.D. Thesis, University of Twente, Netherlands.
[20] Akaike, H., 1974, "A New Look at the Statistical Model Identification," IEEE T. Automat. Contr., 19(6), 716-723.
[21] Hurvich, C. M., and Tsai, C.-L., 1989, "Regression and Time Series Model Selection in Small Samples," Biometrika, 76, 297-307.
[22] Weibull, W., 1951, "A Statistical Distribution Function of Wide Applicability," J. Appl. Mech., 18, 293-297.

Table 1. Maximum Internal Pressures for a Screw Top Can Exposed to a 1273 K Fire

O-ring	Filter Plug	Initial Pressure (Pa)	Upright		Recumbent	
			Full Exposure (Pa)	Half Exposure (Pa)	Full Exposure (Pa)	Half Exposure (Pa)
No	----	0.0	3.20×10^5	3.68×10^5	4.12×10^5	4.31×10^5
Yes	None	0.0	3.99×10^5	3.95×10^5	5.35×10^5	4.96×10^5
	Partial	0.0	5.18×10^5	4.75×10^5	7.33×10^5	6.76×10^5
Yes	None	5.65×10^5	8.59×10^5	6.85×10^5	7.48×10^5	7.06×10^5
	Partial	5.65×10^5	9.85×10^5	7.11×10^5	8.26×10^5	7.06×10^5

Note: Parameters are the presence or absence of the B vial O-ring, presence or absence of partial pluggage of the screw lid thread gap, pressurization of the B vial by radiolytic hydrogen, can orientation (upright or recumbent), and fire exposure (all or half of can exterior). All pressures are gauge pressures.

Fig. 1. B Vial and Screw Top Utility Can

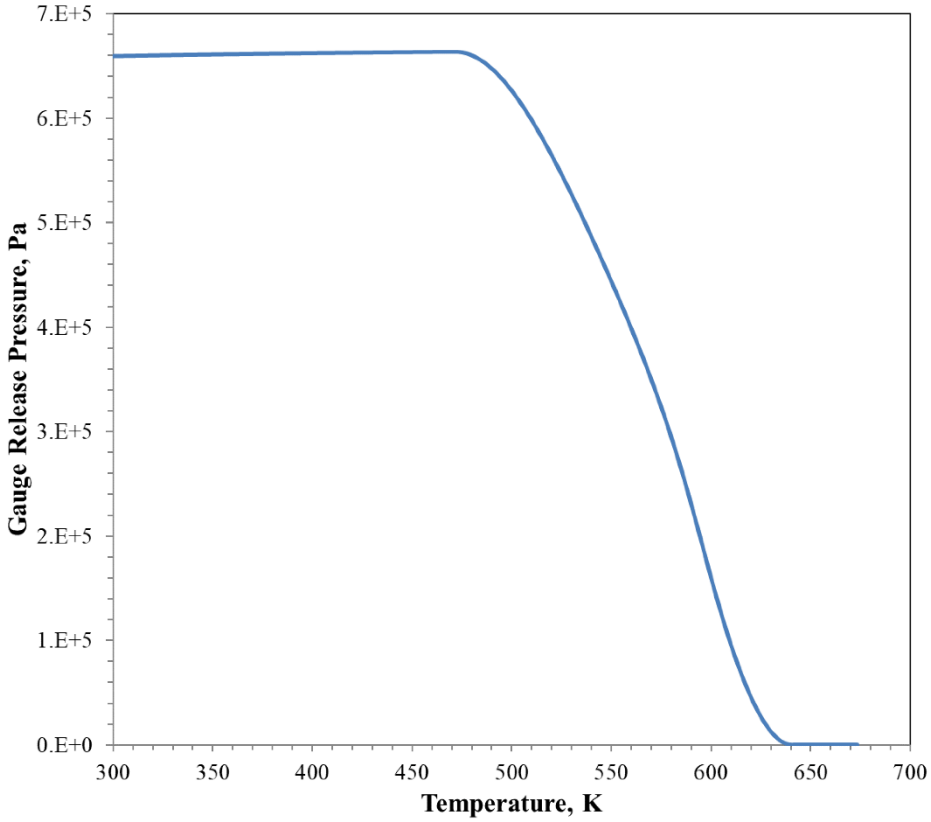

Fig. 2. O-ring Leak Pressure as a Function of Temperature

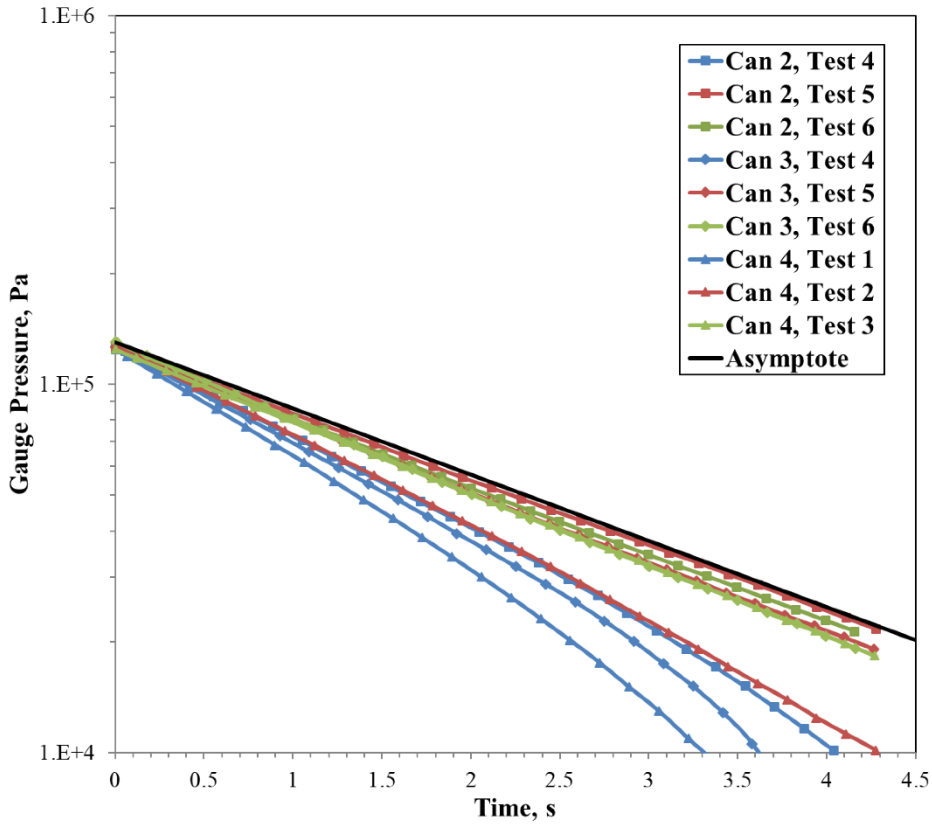

Fig. 3. Variation of Pressure during Screw Top Can Leak Tests

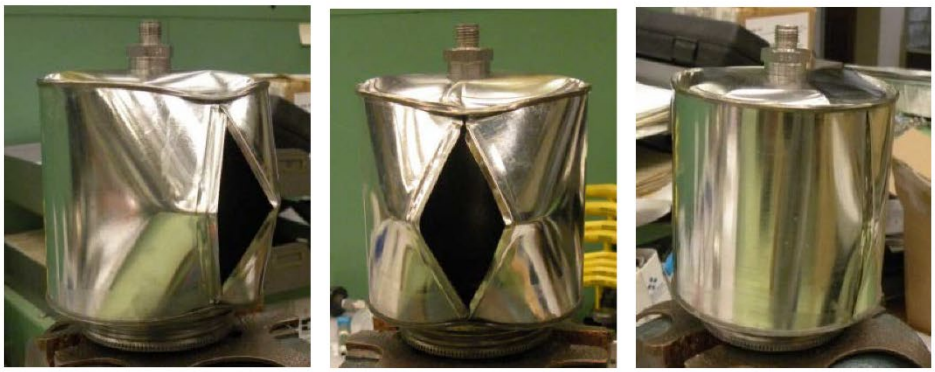

TEST 3 TEST 4 TEST 5

Fig. 4. Screw Top Utility Cans after Bursting

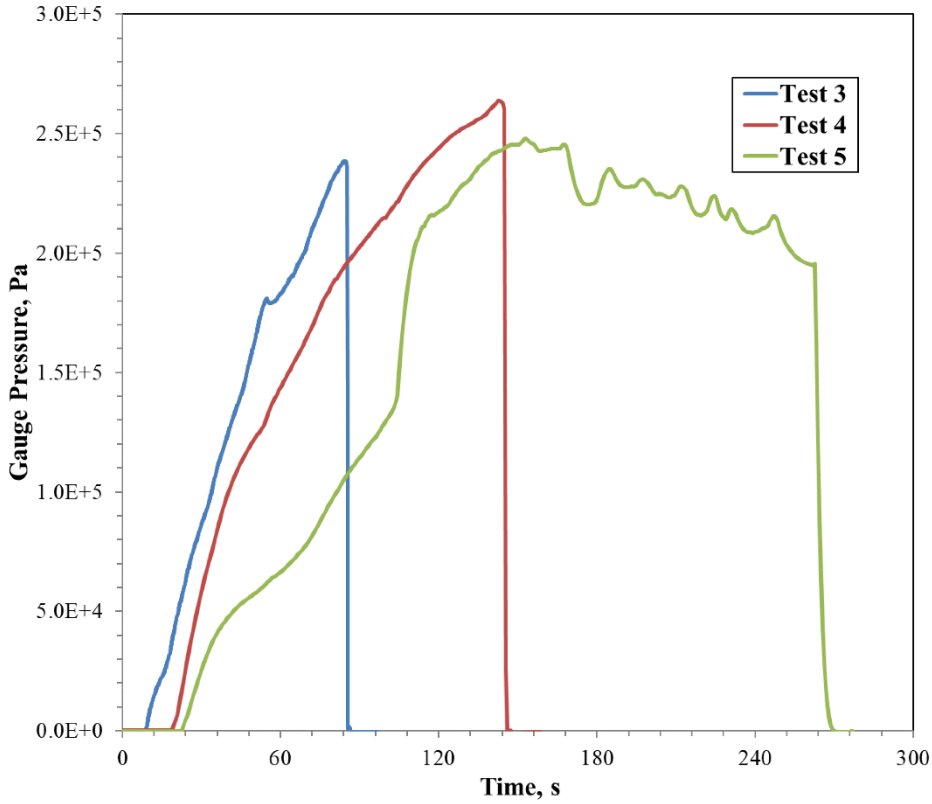

Fig. 5. Variations of Pressure during Screw Top Can Burst Tests

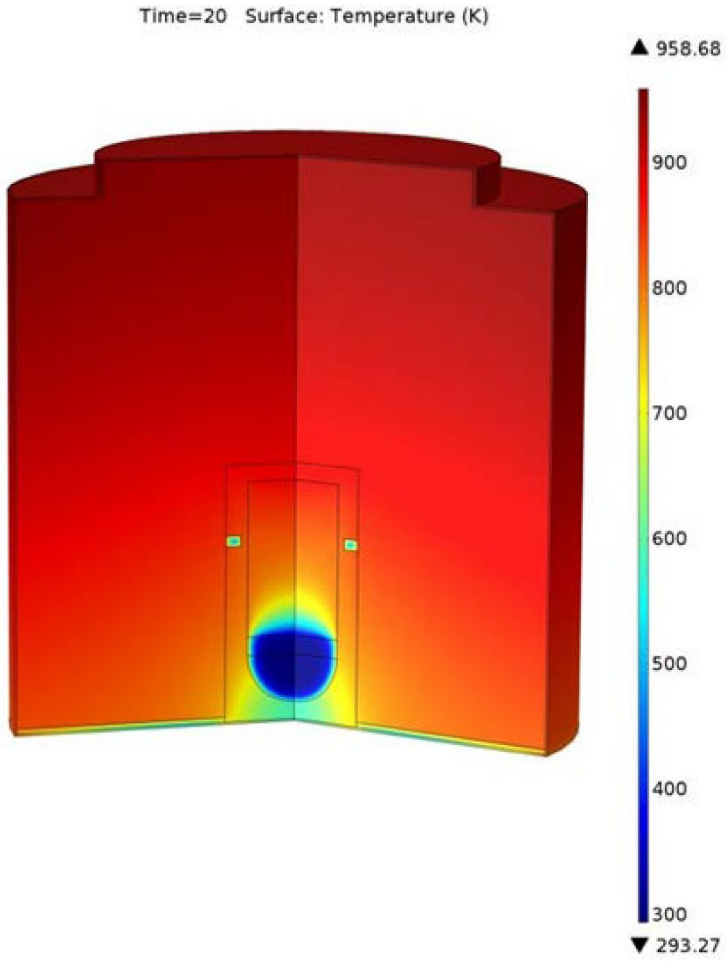

Fig. 6. Temperature Profile for an Upright Screw Top Can with a B Vial and Plastic Bagging, Engulfed by Fire for 20 Seconds

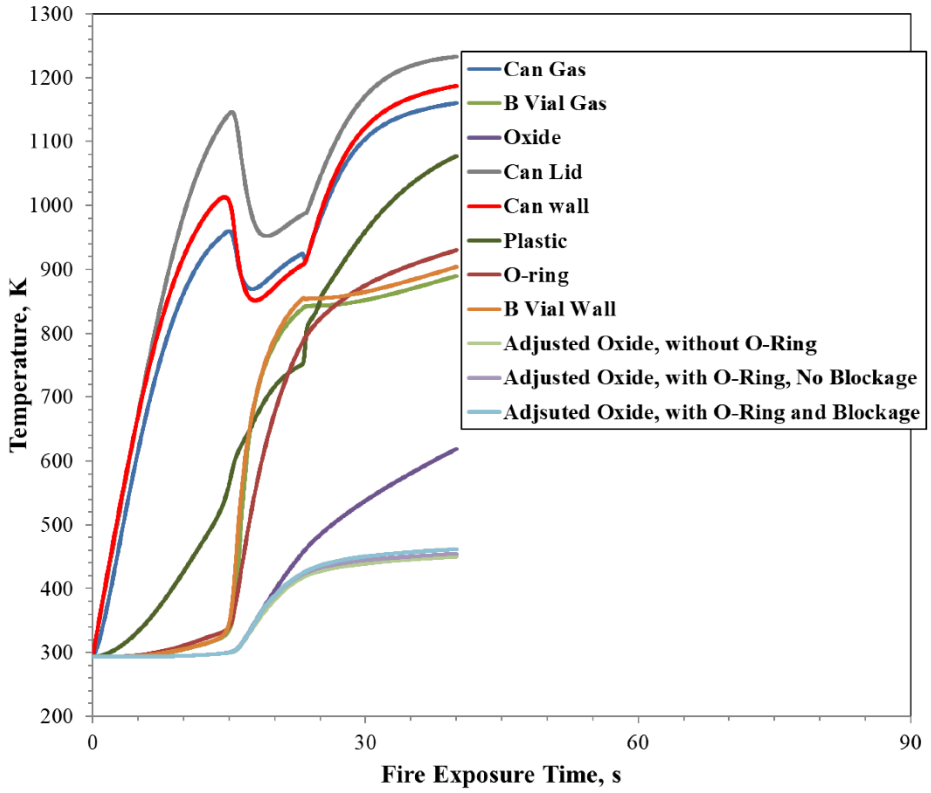

Fig. 7. Temperature Transient for an Upright Screw Top Can Containing a B Vial, Engulfed by a 1273 K Fire

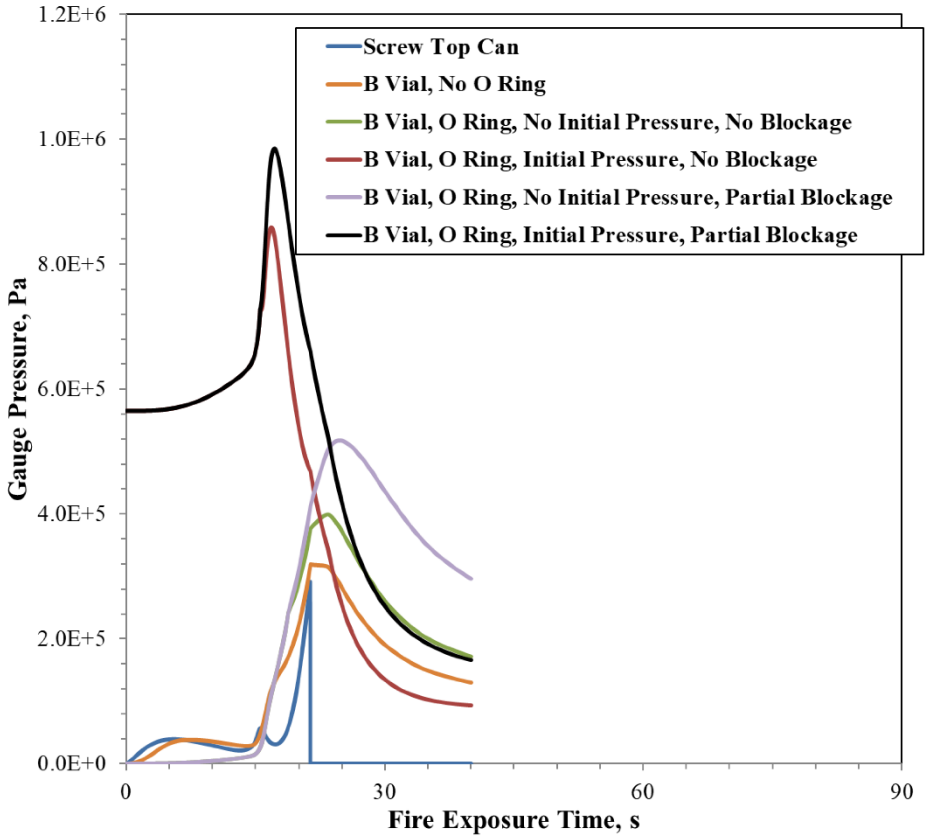

Fig. 8. Pressure Transients for an Upright Screw Top Can Containing a B Vial, Engulfed by a 1273 K Fire